Thin Solid Films 537 (2013) 242–246

Contents lists available at SciVerse ScienceDirect

Thin Solid Films

journal homepage: www.elsevier.com/locate/tsf

Increased crystallinity of octadecylphosphonic acid Langmuir–Blodgett films with an increasing number of layers

F.Z. Zhao [a,1], R. Dey [a,b,2], H.-Y. Nie [a,b,*], W.M. Lau [a,b,c,d,*]

[a] Surface Science Western, The University of Western Ontario, 999 Collip Circle, London, Ontario N6G 0J3, Canada
[b] Department of Physics and Astronomy, The University of Western Ontario, London, Ontario N6A 3K7, Canada
[c] Department of Chemistry, The University of Western Ontario, London, Ontario N6A 5B7, Canada
[d] Chengdu Green Energy and Green Manufacturing Technology R&D Center, Chengdu Development Center of Science and Technology, China Academy of Engineering Physics, Chengdu 610207, People's Republic of China

ARTICLE INFO

Article history:
Received 15 June 2012
Received in revised form 14 April 2013
Accepted 19 April 2013
Available online 3 May 2013

Keywords:
Octadecylphosphonic acid
Langmuir–Blodgett films
molecular headgroups
Si wafer
atomic force microscopy
molecular-resolution images
even-numbered LB films
increased crystallinity

ABSTRACT

We report that contact mode atomic force microscopy (AFM) imaging is useful in revealing crystallinity of octadecylphosphonic acid (OPA) Langmuir–Blodgett (LB) films. On a monolayer OPA LB film prepared on the native oxide of a Si wafer, no molecular-resolution could be obtained. However, molecular-resolution images were obtained on a bilayer surface, a reflection that molecules in the top layer adjust their alkyl chains to accommodate those from below to form a closely packed, OPA headgroup-terminated surface. We demonstrate that with an increasing number of layers, the crystallinity of multilayer OPA LB films improves as molecular-resolution AFM images obtained on even-numbered multilayers reveal that the terminating OPA headgroups form a sheet of hexagonal array.

1. Introduction

With contact mode atomic force microscopy (AFM) operated in air, atomic-resolution images are readily obtained on cleaved mica and highly oriented pyrolytic graphite [1–3], as well as metal films [4,5] deposited on these substrates. Due to the lack of surface defects in such AFM images and the fact that the contact area between the AFM tip and the sample surface is much larger than the dimension of individual atoms, it becomes a consensus that atomic-resolution images obtained in contact mode AFM do not represent the true atomic arrangement of the surface, but, they do reflect the regularity of the atoms collectively sensed by the scanning tip [6,7]. Indeed, in the past two decades, contact mode AFM has proved to be a powerful technique in revealing crystallinity of ordered molecular films such as self-assembled monolayers (SAMs) of alkanethiols on gold [8–16] and Langmuir–Blodgett (LB) films of fatty acids [17–20] on mica and Si. For example, "molecular-resolution" AFM images on thiol SAMs were routinely obtained on alkanethiol SAMs formed on a single crystalline Au (111) film surface [8–15]. For fluorinated disulfides and thiols, molecular resolution was observed on their SAMs on gold film sputtered on cleaved mica [16]. By controlling the loading force, Liu and Salmeron demonstrated that either the monolayer or the gold substrate can be imaged on molecular or atomic resolutions [10]. On the other hand, AFM studies revealed that the crystallinity of fatty acid LB films increases with an increasing number of layers [17–19]. An extensive investigation of quantitative lattice measurements on cadmium arachidate LB films manifests the applicability of AFM in probing the crystallinity of LB films on the molecular scale [17].

Octadecylphosphonic acid (OPA) SAMs formed on oxides are a model system for SAMs [21–23], especially for studying the role of headgroup–substrate interactions in SAM formation [24,25]. For example, an OPA solution in a polar solvent allows monolayer formation on oxides such as cleaved mica and aluminum oxide, where the headgroup–substrate interaction is strong. It has been shown that when a polar solvent (e.g., alcohol) is used, no OPA monolayers form on the native silicon oxide (SiO_2) layer of a Si wafer [26] due to the lack of a strong interaction between the OPA headgroup and the substrate [24]. Rather, an OPA solution in a polar solvent spreads on SiO_2 and results in liquid-like stacks, from which multilayers (crystalline stacks) form slowly (days) [26]. This is a reflection that the liquid phase OPA molecules are highly mobile.

* Corresponding authors at: Surface Science Western, The University of Western Ontario, 999 Collip Circle, London, Ontario N6G 0J3, Canada.
E-mail addresses: hnie@uwo.ca (H.-Y. Nie), llau22@uwo.ca (W.M. Lau).
[1] Present address: School of Physics, Ludong University, Yantai, Shandong 264025, People's Republic of China.
[2] Present address: Department of Electrical and Computer Engineering (Nanotechnology), University of Waterloo, Waterloo, Ontario N2L 3G1, Canada.

0040-6090/$ – see front matter © 2013 Elsevier B.V. All rights reserved.
http://dx.doi.org/10.1016/j.tsf.2013.04.117

It has been demonstrated that weakly bonded OPA SAMs on SiO_2 can be readily formed when using nonpolar solvents having a dielectric constant of ~4 [24]. In such a solvent, the OPA molecules concentrate on the medium surface as a result of the polar headgroups trying to escape from the nonpolar solvent. A contact between the medium and a hydrophilic surface triggers the release of concentrated OPA molecules on the medium surface to the substrate, facilitating a fast growth of (only) SAMs on the substrate. In order to understand how the crystallinity of OPA molecular layers changes when they stack on SiO_2, we adopt the LB technique, which allows formation of both monolayer and multilayer of OPA. In this article, we report that contact mode AFM imaging of the even-numbered multilayer OPA LB films reveals increased crystallinity of the OPA films with an increasing number of layers. We demonstrate that the inability to achieve molecular-resolution images on monolayer OPA LB films is attributable to the lack of strong bonding between the molecular headgroups and the substrate.

2. Experimental section

All OPA [*n*-octadecylphosphonic acid, $CH_3(CH_2)_{17}P(=O)(OH)_2$; Alfa Aesar, Ward Hill, MA] molecular layer samples were prepared on a Si substrate using the LB technique. The Si substrate was cleaned using a UV cleaner (Model T10 × 10/OES, UVOCS Inc., Pa, USA) with a UV lamp emitting light with wavelengths of 185 nm and 254 nm. The 185-nm UV irradiation generates ozone from the ambient air of the chamber. Hydrocarbon contaminants are excited by the 254-nm UV irradiation and oxidized by ozone. The substrate was placed ~3 cm below the UV lamp and the treatment time was 15 min. The cleanliness of the surface was confirmed with water contact angle measurements where the surface was completely wet by de-ionized (DI) water.

The LB films were prepared at room temperature using a KSV 2000 (Finland) system with a Teflon-coated trough operated with double barriers. The trough was filled with DI water with a resistivity of 18 MΩ cm obtained from a purification system (Milli-Q, Millipore, Boston, MA). A 2 mM OPA solution in chloroform was spread on the DI water at room temperature. With the evaporation of the solvent (10 min after solution spreading) and an increase in the surface pressure (measured with the Wilhelmy plate technique) controlled by slowly squeezing the two barriers of the LB trough at a compression speed of 2 cm/min, the OPA molecules form a Langmuir monolayer on the subphase (water) at a surface pressure on the order of 60 mN/m. The Langmuir monolayer was transferred onto the native SiO_2 layer of a Si wafer (on which the hydrophilic OPA headgroups were attached) by pulling out the substrate immersed in the substrate (at a speed of 1 cm/min) to form a monolayer OPA LB film on the support. By dipping the monolayer-coated Si substrate into the subphase, the second monolayer OPA LB film will be transferred onto the surface, in which the alkyl chains of the second monolayer stack on the alkyl chains of the first monolayer OPA LB film. By repeating these processes, multilayer OPA LB films were formed on a Si substrate. When a Langmuir film was being transferred onto the substrate, the system adjusted the barrier position to keep the deposition surface pressure at the pre-set value. As a result of this feed-back mechanism, transfer ratios were close to 1.

All samples were examined using contact mode AFM of an Omicron (Germany) STM/AFM system placed on an anti-vibration floor. Rectangular silicon cantilevers with a nominal spring constant of 0.35 N/m and tip radius of 10 nm were used. Topographic and lateral force images were obtained in air at room temperature, with a loading force of ~1 nN and a scan rate of 30 nm/s. The scanner was calibrated with atomic-resolution images obtained on a cleaved mica surface. The AFM images shown in this article are raw data without any filtering operations. An AFM data processing software (WSxM from Nanotec Electronica S.L. [27]) was used to carry out fast Fourier transform (FT) for the AFM images to reveal their periodic patterns.

3. Results and discussion

Shown in Fig. 1a is an AFM topographic image for a monolayer LB film prepared on SiO_2, from which the thickness of the film was found to be 2.0 nm. Since the extended length of an OAP molecule is 2.5 nm, our results indicate that the alkyl chains in the monolayer LB film tilt 36° away from the surface normal. Shown in Fig. 1b–e are AFM topographic images for a bilayer, a trilayer, a tetralayer and an 18-fold layer OPA LB film on SiO_2, respectively. A profile isolated from the image, as indicated by the insert line, is shown below the image. On these different OPA LB films, we tried high resolution AFM imaging for the purpose of investigating their crystallinity. Fig. 1f is a topographic image obtained on the surface of the Si substrate used as the support for the LB films, showing that the (native oxide layer) SiO_2 surface is amorphous, but smooth. The corrugations observed in Fig. 1f are ~0.3 nm and the root mean square roughness is less than 0.1 nm.

On the surface of an 18-layer OPA LB film, which is terminated by the molecular headgroups, we found that it is rather easy to obtain molecular-resolution images. This is a reflection of the crystallinity of the OPA headgroups terminating the surface of the top layer. Shown in Fig. 2a and b are raw data for topographic and lateral force images, respectively. The magnitude of FT (the insert in the image) of the AFM image is plotted in spatial frequency domain. The three pairs of bright spots in the FT image (the two spots in each pair are symmetric to the center) suggest a hexagonal lattice of the OPA headgroups. The distance between the nearest neighbors (lattice constant) estimated from the filtered image (not shown) obtained with inverse FT is approximately 0.55 ± 0.02 nm, which is in agreement with the molecular density of 0.25 nm^2/molecule for OPA SAMs formed on a cleaved mica surface [21]. The distance between the next-nearest neighbors is 0.98 ± 0.02 nm. We thus infer that the crystallinity seen on the multilayer OPA LB film is a result of the headgroup–headgroup interaction, which renders a rigid and ordered sheet of OPA headgroups.

The two hydroxyl groups in the OPA headgroup result in a headgroup-terminated surface with a high surface energy, which makes the surface reactive and perhaps unstable. We have indeed found that when an OPA solution in alcohol is spread on a Si substrate, the OPA molecules crystallized very slowly (days) from the "liquid-like" phase [26]. The vast majority of the crystalline multilayers were methyl-terminated (odd-numbered) multilayers and no any headgroup-terminated (even-numbered) multilayers beyond bilayer were observed. This previous experimental observation is explained by the fact that a methyl-terminated surface has a much lower surface energy in comparison with a headgroup-terminated surface. From that system, we conclude that OPA molecules are mobile and they form multilayers terminated by their alkyl chains beyond bilayer. This seems to be the stabilization mechanism for eliminating the existence of surfaces with a high surface energy.

On the other hand, in the LB approach, stacking of each monolayer is well controlled in the film transfer process. Surfaces terminated by OPA headgroups, which have a high surface energy and are thus reactive, may be stabilized in part by steric effect by way of formation of a sheet-like structure through hydrogen-bonding of the hydroxyl groups of the headgroups. The other stabilizing mechanism may be adsorption of hydrocarbons and water on the surface to lower the surface energy by some extent. Therefore, it is highly likely that LB multilayers terminated by OPA headgroups become stable in air. Indeed, molecular-resolution images have been obtained on headgroup-terminated LB films [28].

We noticed that there is a special case where a double-chain molecule forms an unconventional double layer with the two alkyl chains extending to opposite directions and the headgroups polymerizing via hydrogen-bonding [29]. Moreover, this process happens at the water–air interface before such a Langmuir layer is transferred to a solid support

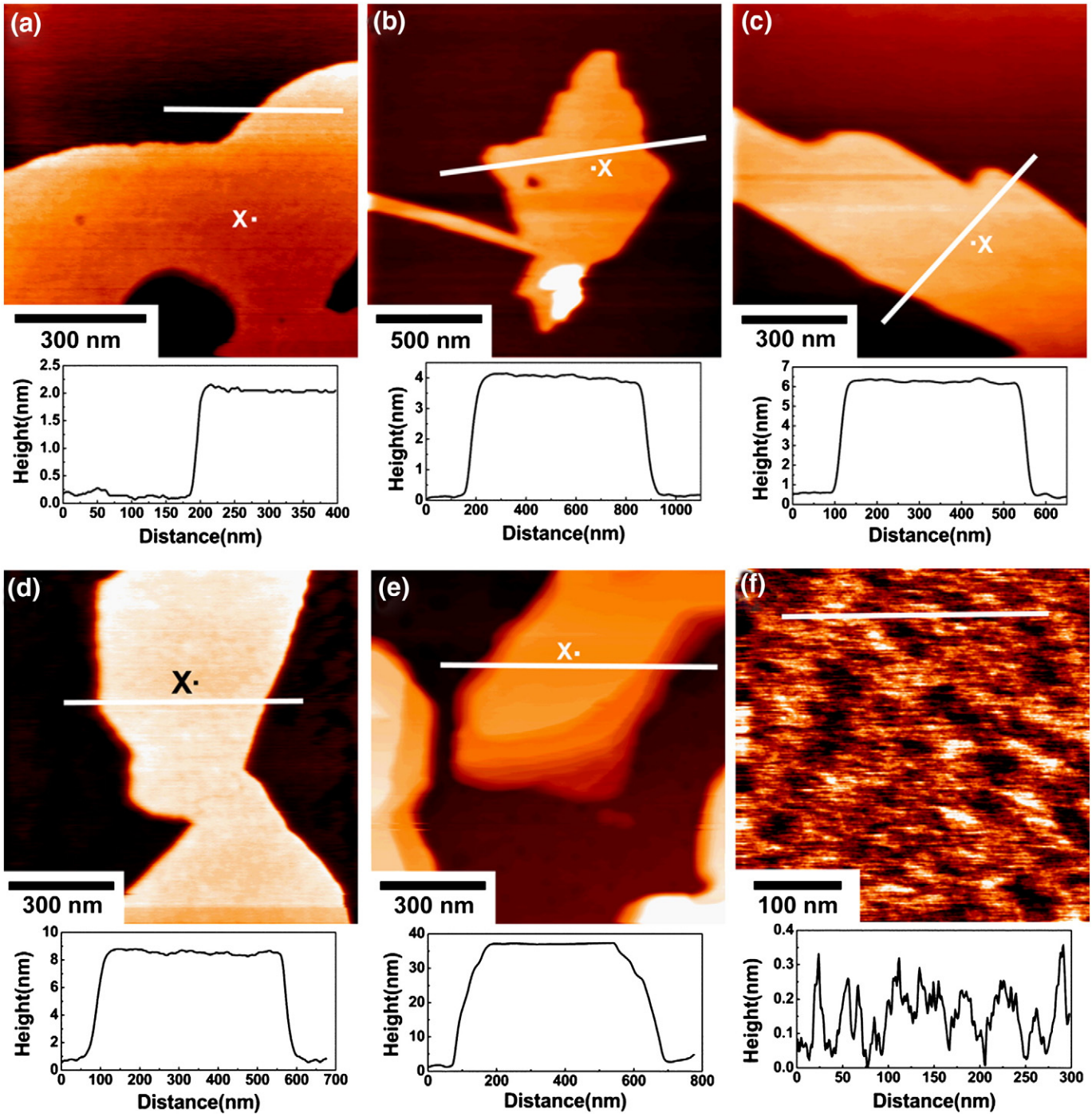

Fig 1. AFM topographic images of (a) monolayer, (b) bilayer, (c) trilayer, (d) tetralayer and (e) 18-layer OPA LB films on a Si substrate, whose surface morphology is shown in (f). The profile for each image is isolated from the insert line to show the LB film thickness for (a)–(e) and the corrugation of the substrate for (f).

(to become a Langmuir–Blodgett film), which is hardly applicable to our case of OPA molecules.

Shown in Fig. 3a is a friction force image obtained on the monolayer LB film surface, which is featureless. The FT of this image inserted in the image confirms that there are no specific structures detected. Therefore, on a monolayer OPA LB film prepared on SiO_2, we could not obtain molecular-resolution images. This experimental result may be explained by two possibilities: (a) the crystallinity of the monolayer is limited by the underlying morphology of the substrate and (b) the molecules are not strongly bonded to the substrate so that the molecules move, yielding to the contact force exerted from the AFM tip. In the first case, the OPA headgroups follow the contour of the surface morphology of the substrate, with the alkyl chains sticking out. It may appear that the amorphous nature of the substrate is responsible for the lack of molecular resolution in our AFM image for the monolayer OPA LB film formed on SiO_2. This is in agreement with the observations of Peltonen et al. made on octadecenoic acid LB films prepared on a glass substrate — only after five layers, they started to observe the lattice of the molecules [30]. On the other hand, Schönherr and Vancso reported that they readily obtained molecular-resolution AFM images on SAMs of thiols prepared on a sputtered gold film [16]. The sputtered gold film is much rougher than a mirror-polished Si wafer like the one we used as the

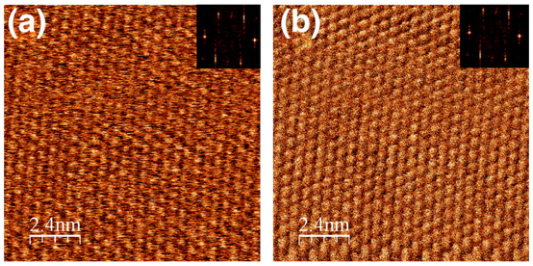

Fig. 2. Raw topographic (a) and lateral force (b) images (scan area: 12 nm × 12 nm) obtained on an 18-layer OPA LB film showing molecular resolution. The insert shows Fourier transform of the AFM image. The height range of the topographic image is 0.16 nm.

substrate for our OPA LB films. The reason for the hexagonal lattice observed by AFM on SAMs of thiols formed on the sputtered gold film is attributed to chain–chain interactions [16].

An important point to make on the observed molecular resolution for the thiol SAMs is that the molecules are strongly bonded on the gold film by S–Au linkage. By contrast, in our monolayer OPA LB film prepared on SiO_2, the molecules are only weakly bonded on the surface. We have verified that the bonding mode of OPA molecules on SiO_2 is hydrogen-bonding [24,25]. Therefore, we must consider the second possibility: that the lack of molecular resolution on the OPA monolayer LB film is perhaps due to the weak interaction between the molecular headgroup and the substrate. One can imagine that when their chains are dragged by the AFM tip, the OPA molecules move a short distance without resisting strongly to the traversing tip. This (lack of) interaction between the molecules and the AFM tip hence results in a featureless morphology (Fig. 3a). According to our experimental results presented above, it appears that the crystallinity of layered molecular structure can be probed by contact mode AFM only if the molecules are strongly attached to a substrate. Our inability to obtain molecular-resolution images on a monolayer OPA LB film is thus attributed to the lack of strong attachment of the molecules to the substrate.

When stacking another layer of OPA molecular film on the monolayer OPA LB film, the alkyl chains in the second layer make contact with those in the first layer, forming a bilayer with the headgroups

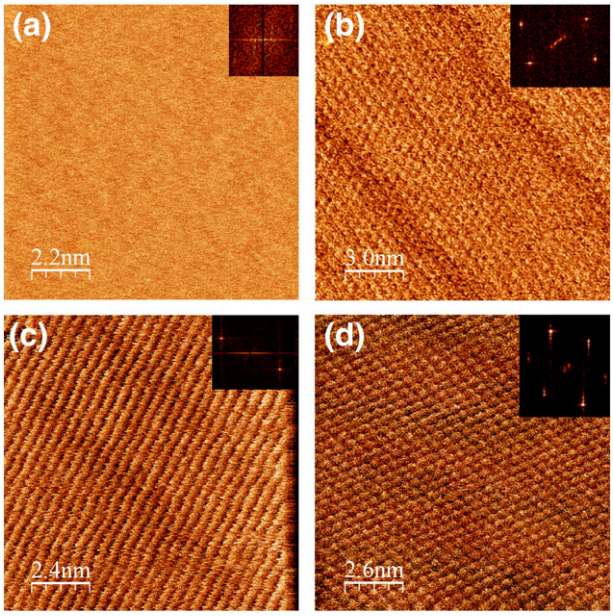

Fig. 3. Raw lateral force image obtained on (a) monolayer, (b) bilayer, (c) trilayer and (d) tetralayer of OPA LB films formed on SiO_2. The images in a–d were obtained in an area of 11 nm × 11 nm, 15 nm × 15 nm, 12 nm × 12 nm and 13 nm × 13 nm, respectively. The insert shows Fourier transform of the image.

terminating the surface. Assisted by the flexibility of the alkyl chains as well as hydrogen-bonding between the hydroxyl groups from adjacent OPA headgroups, the OPA headgroups in the second layer tend to form a sheet-like structure. As shown in Fig. 3b, we were able to merely achieve molecular-resolution AFM images on the OPA headgroup-terminated bilayer surface. Interestingly, the FT in the insert of Fig. 3b shows two pairs of bright spots, with another pair of spots too weak to be seen. The FT results clearly show that the lattice of the OPA headgroups is distorted. The bright spots are more like a rectangular lattice. The two nearest neighbor distances are 0.54 ± 0.01 and 0.48 ± 0.01 nm. The implication of this observation of a distorted lattice is two-fold. On one hand, it proves that the molecular headgroups terminating the bilayer surface form a regular array. This requires that the alkyl chains of the top layer adjust to those of the underneath monolayer. This way, the roughness of the substrate has less effect on the terminating OPA headgroups in the second layer. This is perhaps the mechanism for OPA molecules in multilayer LB films to self-align. On the other hand, comparisons of the FT patterns of the AFM images for the bilayer (Fig. 3b) and the 18-layer (Fig. 2) OPA LB films show that the crystallinity of OPA LB films increases with an increasing number of layers.

When another OPA molecular layer is added to the bilayer, a trilayer is formed, with the alkyl chains terminating the surface. In comparison to the monolayer on SiO_2, the OPA headgroups in the third layer are attached to the array of OPA headgroups terminating the second layer, which is believed to be smoother than SiO_2 (the surface of the Si substrate). As shown in Fig. 3c, on the trilayer surface, a stripe-like feature was observed. The FT in the insert in Fig. 3c shows a pair of spots reflecting the stripes seen in the AFM image. The stripe pitch is 0.45 ± 0.02 nm.

In comparison to the featureless AFM image (Fig. 3a) obtained on OPA monolayer LB films, the stripe-like feature (Fig. 3c) obtained on the trilayer suggests some difference between the two LB films. Both the monolayer and the trilayer are terminated by the alkyl chains of OPA molecules. The difference lies in the surface that the molecules are attached to: it is SiO_2 for the monolayer and an array of OPA headgroups for the trilayer, which may be reflected in differences detected by the contact mode AFM. As previously mentioned in this article, the lack of molecular resolution in AFM images obtained on monolayer OPA LB films is attributable to the weak attachment of OPA headgroups to SiO_2 surface. In the trilayer case, OPA molecules in the third layer are attached to the array OPA headgroups of the second layer. The interactive strength between the second-layer and the third-layer OPA headgroups is most likely that of hydrogen-bonding. Yet, we observed stripe-like features, indicating that there is a directional restriction of the movement of the OPA molecules. We explain the stripe-like features by assuming that the molecules establish stronger van der Waals forces in a certain direction, along which the molecular chains resist the drag of the scanning AFM tip. This is the direction with contrast of friction seen in Fig. 3c. For the direction perpendicular to this specific direction, the distance is a little larger, making the molecules have less resistance to the scanning AFM tip. This renders no friction force contrast in that direction. If this is indeed the mechanism for the observed stripe-like AFM image (Fig. 3c) on a trilayer surface, then for any further odd-numbered multilayers, one expects to obtain stripe-like features similar to the one shown in Fig. 3c. However, this remains to be tested since we could not find odd-numbered multilayers beyond trilayer.

When attaching a monolayer on a trilayer, a tetralayer OPA LB film is formed with the OPA headgroup terminating the surface. Shown in Fig. 3d is an AFM image obtained on the surface of a tetralayer OPA LB film. The FT of the molecular-resolution AFM image shows three pairs of bright spots, from which we have a distorted hexagonal lattice with two nearest neighbor distances of 0.51 ± 0.01 and 0.45 ± 0.01 nm.

Comparisons of the AFM images and the corresponding FT results among the bilayer, tetralayer and 18-layer OPA LB films clearly show that the crystallinity of OPA LB films increases with an increasing number of layers stacked. We stress that the rigidity of the surface terminated

by the OPA headgroups is key for the AFM tip/cantilever ensemble to be able to sense the lattice formed by the OPA molecules.

Our AFM results on the headgroup-terminated LB films are in agreement with those obtained on fatty acid LB films [28]. However, for the alkyl chain-terminated LB films, our study provides insights for understanding how molecular-resolution AFM images may be achieved on a monolayer: it requires that the molecules be strongly attached to the "substrate" so that their crystallinity can be sensed by a dragging AFM tip imposing a contact area much larger than the size of the molecules "resolved" by the AFM image. This aspect apparently might not have been noticed, largely because the majority of work in this area has been carried out on monolayers in which the molecular headgroups are strongly bonded to the substrate. Since the bilayer has the "crystalline" surface of OPA molecular headgroups, the AFM results obtained on trilayer further support the idea that lack of strong interactions between the molecular headgroup and the "substrate" prevents imaging of hexagonal lattice of the molecular chains. This is reasonable because AFM, in principle, probes the surface via interactions between the AFM tip and the surface of the sample. From our results, we emphasize that molecular-resolution images obtained in contact mode are a reflection of the convolution of the crystallinity of the molecules and the interaction between the dragging AFM tip and the response of the molecules.

4. Conclusions

Contact mode AFM was used to study OPA LB films on the native oxide surface of a Si wafer, where the OPA molecular headgroups in the first layer are weakly attached to the substrate. Its inability to obtain molecular-resolution AFM images on a monolayer OPA LB film is attributed to the weak interaction between the headgroup and the substrate. We elucidate that a molecular-resolution image is a reflection of the formation of a sheet-like structure of closely packed headgroups. Our results confirmed that with an increasing number of layers, the crystallinity of multilayer OPA LB films is enhanced and eventually a hexagonal lattice is realized.

Acknowledgments

The authors are grateful for support from Surface Science Western. This work was partially supported by the Leaders Opportunity Fund from Canada Foundation for Innovation awarded to W.M.L. W.M.L. thanks the China Academy of Engineering Physics, Beijing Computation Science Research Center, and Chengdu Science & Technology Development Center for their support. F.Z.Z. was supported in part by the Educational Commission of Shandong Province, China (Project No. J08LI04) and Innovation Project of Ludong University (Project No. LY20062802).

References

[1] T.R. Albrecht, C.F. Quate, J. Appl. Phys. 62 (1987) 2599.
[2] S. Alexander, L. Hellemans, O. Marti, J. Schneir, V. Elings, P.K. Hansma, Matt Longmire, J. Gurley, J. Appl. Phys. 65 (1989) 164.
[3] H.Y. Nie, T. Shimizu, H. Tokumoto, J. Vac. Sci. Technol. B 12 (1994) 1843.
[4] T. Fukuma, K. Kobayashi, T. Horiuchi, H. Yamada, K. Matsushige, Appl. Phys. A 72 (2001) S109.
[5] Y. Gan, Surf. Sci. Rep. 64 (2009) 99.
[6] J.B. Pethica, Phys. Rev. Lett. 57 (1986) 3235.
[7] M.R. Jarvis, R. Pérez, M.C. Payne, Phys. Rev. Lett. 86 (2001) 1287.
[8] C.A. Alves, E.L. Smith, M.D. Porter, J. Am. Chem. Soc. 114 (1992) 1222.
[9] L.A. Bumm, J.J. Arnold, T.D. Dunbar, D.L. Allara, P.S. Weiss, J. Phys. Chem. B 103 (1999) 8122.
[10] G.-Y. Liu, M.B. Salmeron, Langmuir 10 (1994) 367.
[11] X.J. Yang, S.S. Perry, Langmuir 19 (2003) 6135.
[12] G. Nelles, H. Schönherr, M. Jaschke, H. Wolf, M. Schaub, J. Küther, W. Tremel, E. Bamberg, H. Ringsdorf, H.-J. Butt, Langmuir 14 (1998) 808.
[13] H.I. Kim, T. Koini, T.R. Lee, S.S. Perry, Langmuir 13 (1997) 7192.
[14] A. Lio, C. Morant, D.F. Ogletree, M. Salmeron, J. Phys. Chem. B 101 (1997) 4767.
[15] A. Lio, D.H. Charych, M. Salmeron, J. Phys. Chem. B 101 (1997) 3800.
[16] H. Schönherr, G.J. Vancso, Langmuir 13 (1997) 3769.
[17] D.K. Schwartz, J. Garnaes, R. Viswanathan, S. Chiruvolu, J.A.N. Zasadzinski, Phys. Rev. E 47 (1993) 452.
[18] J.A. Zasadzinski, R. Viswanathan, L. Madsen, J. Garnaes, D.K. Schwartz, Science 263 (1994) 1726.
[19] D.Y. Takamoto, E. Aydil, J.A. Zasadzinski, A.T. Ivanova, D.K. Schwartz, T.L. Yang, P.S. Cremer, Science 293 (2001) 1292.
[20] H.H. Li, G.Z. Mao, K.Y.S. Ng, Thin Solid Films 358 (2000) 62.
[21] J.T. Woodward, A. Ulman, D.K. Schwartz, Langmuir 12 (1996) 3626.
[22] B.R.A. Neves, M.E. Salmon, P.E. Russell, E.B. Troughton Jr., Langmuir 16 (2000) 2409.
[23] W. Gao, L. Dickinson, C. Grozinger, F.G. Morin, L. Reven, Langmuir 1 (2) (1996) 6429.
[24] H.-Y. Nie, M.J. Walzak, N.S. McIntyre, J. Phys. Chem. B 110 (2006) 21101.
[25] H.-Y. Nie, Anal. Chem. 82 (2010) 3371.
[26] H.-Y. Nie, M.J. Walzak, N.S. McIntyre, Langmuir 18 (2002) 2955.
[27] I. Horcas, R. Fernandez, J.M. Gomez-Rodriguez, J. Colchero, J. Gomez-Herrero, A.M. Baro, Rev. Sci. Instrum. 78 (2007) 013705.
[28] D.K. Schwartz, R. Viswanathan, J.A.N. Zasadzinski, J. Phys. Chem. 96 (1992) 10444.
[29] Q. Huo, S. Russev, T. Hasegawa, J. Nishijo, J. Umemura, G. Puccetti, K.C. Russell, R.M. Leblanc, J. Am. Chem. Soc. 122 (2000) 7890.
[30] J.P.K. Peltonen, P. He, J.B. Rosenholm, J. Am. Chem. Soc. 114 (1992) 7637.